ADVANCED NUMERICAL COMPUTATION OF TWO-DIMENSIONAL TIME-DEPENDENT FREE CONVECTION IN CAVITIES

K. Küblbeck,* G. P. Merker† and J. Straub*

Abstract – A two-dimensional time-dependent numerical computation method has been developed to determine laminar free convection in closed cavities and forced convection in ducts and open cavities. The transport equations for energy and vorticity are solved with the aid of the ADI-method, but the more recently established method of cyclic reduction is applied to the Poisson equation. The resulting implicit method remains stable up to a Rayleigh number of 10^{12}. Due to the acceptable large time step, the method is particularly qualified for transient problems with extremely slow changing properties. A transformation relation, $q(x, \varepsilon)$, is proposed for sufficiently accurate determination of thermal and hydrodynamic boundary layers near the vertical side walls in cavities. The benefit of the present numerical computation technique has been demonstrated by solving two problems of free convection in a rectangular cavity, namely with differentially but uniformly heated side walls and with only one side wall non-uniformly heated.

NOMENCLATURE

a,	thermal conductivity;
$a(x), b(x), c(x)$,	functions;
A_x, A_y, B_x, B_y,	derivatives of the transformation equation;
d/dt,	total differential;
$\mathbf{e} = (0, 1)$,	unit vector;
$f_{i,j}$,	coefficient;
$f(x, y)$,	function;
g,	gravity;
$Gr = \dfrac{gL^3}{v^2} \cdot \beta \cdot (T - T_0)$,	Grashof number;
h,	decomposition rate;
H,	height of cavity;
I,	grid point notation in x-direction;
J,	grid point notation in y-direction;
k,	exponent of convergence parabel;
L,	length of cavity;
$Pr = v/a$,	Prandtl number;
p,	pressure;
$p(x), q(y)$,	transformation relation;
$Ra = Gr \cdot Pr$,	Rayleigh number;
$R_{i,j}, S_{i,j}, T_{i,j}, U_{i,j}$,	coefficients of resulting matrices;
Re,	Reynolds number;
Re_z,	cell-Reynolds number (23);
S,	linear deformation parameter;
t,	time;
T,	temperature;
$\mathbf{u} = (u, v)$,	velocity;
W,	width of cavity;
$\mathbf{x} = (x, y)$,	Cartesian coordinates.

Greek symbols

α,	dummy parameter;
β,	coefficient of thermal expansion;
Γ,	dummy variable;
$\dfrac{\delta}{\delta p}, \dfrac{\delta}{\delta q}$,	indicates space-centred approximations;
ε,	nonlinear deformation parameter;
$\theta = (T - T_c)/(T_h - T_c)$,	non-dimensional temperature;
λ,	thermal conductivity;
v,	kinematic viscosity;
ρ,	density;
$\tau = at/H^2$,	non-dimensional time (Fourier number);
ψ,	stream function;
ω,	vorticity;
∇,	Nabla operator;
∇^2,	Laplace operator.

Subscripts

*,	non-dimensional variable;
n,	time step;
0,	reference quantity.

Superscripts

c,	cold;
h,	hot;
i, j,	spatial grid points;
0,	initial value;
w,	wall.

*Lehrstuhl A für Thermodynamik, Technische Universität München, 8000 Munich 2, P.O. Box 202420, Germany.
†MTU — München GmbH, 8000 Munich 50, P.O. Box 500640, Germany.

1. INTRODUCTION

For many heat transfer problems, the governing differential equations are far too complicated to be solved by analytical techniques. Therefore, a detailed and sufficiently accurate description of the resulting temperature and velocity patterns can only be achieved by numerical computation. Well known examples are the heat waste of hot fluid through internal heat transfer processes in thermal energy storage systems (Schöll [1], Straub et al. [2]), temperature equalization processes in air-conditioning systems (Moog [3]) and seasonal temperature distributions in lakes due to eddy and thermal mixing processes (Bloß [4]).

Especially in the field of engineering, it is common practice to describe complicated physical problems with simple and often crude models, with the advantages that an analytical or numerical solution can be easily derived. As these models are based either on some drastic simplifications of the full governing equations or on simple overall energy balances with the unknown transfer processes approximated by semi-empirical correlations the results are often limited and of modest value.

On the other hand, analytical solutions of the full nonlinear basic equations have become known for only a very few problems [5]. In recent years the method of matched asymptotic expansions has been developed (Van Dyke [6], Nayfeh [7]), and successfully applied to free convection problems in shallow cavities (Cormack et al. [8]).

Experimental investigations are usually restricted to the study of laboratory models whereby the similarity conditions are often hard to meet.

Therefore, for most advanced problems the only acceptable solution method is a numerical computation technique. The literature on numerical computation methods has been rapidly expanding in recent years but very few of these methods are of moderate value as the convergence and stability criteria are not sufficiently satisfied in fluid problems with high Rayleigh numbers of 10^6 and more, or if the convergence and stability criteria are fully satisfied, the time step and/or the mesh size becomes so small that the needed computation time is far beyond any reasonable limit. Hence, there is still a strong demand for fast numerical computation techniques which avoid these difficulties.

For instance, steady state numerical methods for recirculating flows which have appeared in the literature in recent years are usually restricted to low Rayleigh number flows and become instable for $Ra > 10^6$ (Rubel and Landis [9], Fromm [10, 11], De Vahl Davis [12], McGregor and Emery [13]). The transient method by Wilkes [14] for elliptical differential equations is also restricted to $Ra < 10^5$.

A review of various numerical techniques has been given by Torrance [15]. He also points to the problem of artificial viscosity which leads to non-energy and/or continuity conserving formulas and, therefore, to erroneous results. The more recently developed methods are reviewed in the excellent book by Roache [16].

In this paper, a fast numerical computation method for transient two-dimensional problems of free and forced convection is described.

2. MATHEMATICAL FORMULATION

Neglecting the dissipation and pressure term in the energy equation one obtains, subject to the usual Boussinesq approximation, the governing equation for an incompressible fluid with constant properties (except density) (see e.g. [17, 18])

$$\nabla \mathbf{u} = 0, \tag{1}$$

$$\frac{d\mathbf{u}}{dt} = -\frac{1}{\rho_0}\nabla p + \nu\nabla^2\mathbf{u} + g\mathbf{e}\frac{\rho_0 - \rho}{\rho}, \tag{2}$$

$$\frac{dT}{dt} = a\nabla^2 T, \tag{3}$$

where the equation of state is reduced to a simple density–temperature relation

$$\frac{\rho}{\rho_0} = \frac{1}{1 + \beta(T - T_0)}. \tag{4}$$

For two-dimensional problems, it is convenient to define a stream function ψ which satisfies the equation of continuity identically

$$u = \frac{\partial\psi}{\partial y}, \quad v = -\frac{\partial\psi}{\partial x}. \tag{5}$$

Elimination of the pressure from the equation of motion and introducing the vorticity ω gives

$$\omega = \frac{\partial v}{\partial x} - \frac{\partial u}{\partial y}. \tag{6}$$

The equations of motion are reduced to the transport equation of vorticity

$$\frac{d\omega}{dt} = \nu\nabla^2\omega + g\beta\frac{\partial T}{\partial x}. \tag{7}$$

Before proceeding further, it is convenient to bring these equations into dimensionless form. With

$$(x^*, y^*) = (x, y)/L,$$
$$(u^*, v^*) = (u, v)/u_0,$$
$$p^* = p/\rho_0 u_0^2,$$
$$\tau = a \cdot t/L^2,$$
$$\theta = (T - T_c)/(T_h - T_c),$$

one obtains

$$\omega = -\nabla^2\psi, \tag{8}$$

$$\frac{d\omega}{d\tau} = Pr \cdot \nabla^2\omega + Gr \cdot Pr^2 \cdot \frac{\partial\theta}{\partial x}, \tag{9}$$

$$\frac{d\theta}{d\tau} = \nabla^2\theta, \tag{10}$$

where the asterisks have been omitted to simplify matters.

As there is no characteristic velocity in pure free convection problems we assume $u_0 = a/L$. Hence the Reynolds number $Re = u_0 L/v$ becomes identical with the Prandtl number, $Pr = a/v$ and the Péclet number, $Pe = u_0 L/a$, becomes equal to unity.

Equations (5) and (8)–(10) are the governing differential equations for free convection problems. To solve this set of equations is not a simple matter as the vorticity equation is coupled to the elliptic Poisson equation through the nonlinear convection terms.

For a numerical solution procedure these equations are usually directly transformed into finite difference equations with the aid of a proper differencing scheme. But to account for the vertical boundary layers near the side walls one would have to introduce an extremely dense grid which leads to a tremendous number of algebraic equations having to be solved. Generally, this situation can be improved either by mapping the flow area under consideration with a non-equidistant grid, i.e. small mesh size in the boundary region and larger grid distances in the core flow region or by introducing suitable transformation equations, $p(x)$ and $q(y)$, which accumulate the grid points in the boundary layer region. With a proper transformation equation, the second method allows arbitrary boundary layer decomposition and is, in our experience, simpler to deal with than non-equidistant mesh sizes.

With arbitrary transformation relations $p(x)$ and $q(y)$ one obtains for the first derivative of a dummy variable Γ

$$\frac{\partial \Gamma}{\partial x} = \frac{\partial \Gamma}{\partial p} \cdot \frac{\partial p}{\partial x} \equiv \frac{\partial \Gamma}{\partial p} \cdot A_x,$$

$$\frac{\partial \Gamma}{\partial y} = \frac{\partial \Gamma}{\partial q} \cdot \frac{\partial q}{\partial y} \equiv \frac{\partial \Gamma}{\partial q} \cdot A_y \tag{11}$$

and, from this, for the second derivatives

$$\frac{\partial^2 \Gamma}{\partial x^2} = \frac{\partial^2 \Gamma}{\partial p^2} \cdot A_x^2 + \frac{\partial \Gamma}{\partial p} \cdot B_x, \tag{12}$$

$$\frac{\partial^2 \Gamma}{\partial y^2} = \frac{\partial^2 \Gamma}{\partial q^2} \cdot A_y^2 + \frac{\partial \Gamma}{\partial q} \cdot B_y.$$

Substituting (11) and (12) into (8)–(10) one obtains the following set of transformed equations

$$-\omega = A_x^2 \frac{\partial^2 \psi}{\partial p^2} + B_x \frac{\partial \psi}{\partial p} + A_y^2 \frac{\partial^2 \psi}{\partial q^2} + B_y \frac{\partial \psi}{\partial q}, \tag{13}$$

$$\frac{\partial \omega}{\partial \tau} + A_x u \frac{\partial \omega}{\partial p} + A_y \cdot v \frac{\partial \omega}{\partial q}$$

$$= Pr \cdot \left(A_x^2 \frac{\partial^2 \omega}{\partial p^2} + A_y^2 \frac{\partial^2 \omega}{\partial q^2} \right)$$

$$+ Pr \cdot \left(B_x \frac{\partial \omega}{\partial p} + B_y \frac{\partial \omega}{\partial q} \right)$$

$$+ Gr \cdot Pr^2 A_x \cdot \frac{\partial \theta}{\partial p}, \tag{14}$$

$$\frac{\partial \theta}{\partial \tau} + A_x u \frac{\partial \theta}{\partial p} + A_y \cdot v \frac{\partial \theta}{\partial q} = A_x^2 \frac{\partial^2 \theta}{\partial p^2} + A_y^2 \frac{\partial^2 \theta}{\partial q^2}$$

$$+ B_x \frac{\partial \theta}{\partial p} + B_y \frac{\partial \theta}{\partial q}, \tag{15}$$

$$u = A_y \frac{\partial \psi}{\partial q}, \quad v = -A_x \frac{\partial \psi}{\partial p}. \tag{16}$$

It should be noted that the non-transformed equations are easily re-established by setting

$$A_x = A_y = 1 \quad \text{and} \quad B_x = B_y = 0.$$

Therefore, the transformation relation can be simply switched off for problems where it is not needed.

3. NUMERICAL PROCEDURE

3.1. Energy and vorticity equation

The energy and vorticity transport equations are of the same 'elliptic type'. They pose a boundary value problem and can be treated with one of the integration techniques briefly outlined in this chapter.

Well established explicit methods are the Euler-method (one-step), Heun-method (two-step) and Runge–Kutta-method (multi-step). To satisfy the strong stability criteria of these explicit methods extremely small time steps are usually required which lead to considerable computation times. Hence, these methods are not suitable for slow changing transient processes. For instance, applying the Euler-method to the problem considered in Chapter 4.1 leads to a computation to real time rate of approximately 10:1.

Some success is gained by introducing semi-analytical methods. In two-dimensional transient problems, the differential equations are separated into two of three independent variables. The resulting coupled ordinary differential equations are then solved with the procedure by Runge–Kutta or Stoer–Bulirsch [19], respectively. These methods are very accurate but still time consuming due to the large number of coupled differential equations.

3.1.1. The ADI-method.
Probably, the best known and widely used implicit method is the Crank–Nicolson method. Contrary to the point-by-point solution technique of the explicit methods, simple implicit methods use advance values in the spatial derivatives, thereby requiring the simultaneous solution of a large number of algebraic equations. Furthermore, application of implicit methods to two-dimensional problems, leads to a set of equations which can be solved by inversion of the resulting pentagonal matrix.

Contrary to this, the ADI-method (alternating direction implicit method) by Peaceman and Rachford [20] splits the time step to obtain a multi-dimensional implicit method which requires only the inversion of a

tridiagonal matrix. This tridiagonal matrix can be solved with the Thomas algorithm [21] which is merely a special adaptation of the Gaussian elimination procedure; see Richtmeyer and Morton [22]. Credit is given to the ADI-method because relatively large time steps are permitted. Furthermore, it has a second order accuracy of $O(\Delta t^2,\ \Delta x^2,\ \Delta y^2)$ and its 'weak' stability conditions are easy to satisfy. (For further details see Roache [16].)

Equation (14) and (15) may be written in a combined form for a dummy variable as

$$\frac{\partial\Gamma}{\partial\tau} + A_x \cdot u \cdot \frac{\partial\Gamma}{\partial p} + A_y \cdot v \cdot \frac{\partial\Gamma}{\partial q}$$

$$= \alpha\left(A_x^2\frac{\partial^2\Gamma}{\partial p^2} + A_y^2\frac{\partial^2\Gamma}{\partial q^2} + B_x\frac{\partial\Gamma}{\partial p} + B_y\frac{\partial\Gamma}{\partial q}\right) + \beta, \quad (17)$$

with $\alpha = 1$ and $\beta = 0$ for the energy and $\alpha = Pr$ and $\beta = GrPr^2 A_x\partial\theta/\partial p$ for the vorticity equation.

Splitting the time step $\Delta\tau$ leads to

$$\frac{\Gamma^{n+1/2} - \Gamma^n}{\Delta\tau/2} + A_xu^n\frac{\delta\Gamma^{n+1/2}}{\delta p} + A_yv^n\frac{\delta\Gamma^n}{\delta q}$$

$$= \alpha\left(A_x^2\frac{\delta^2\Gamma^{n+1/2}}{\delta p^2} + A_y^2\frac{\delta^2\Gamma^n}{\delta q^2}\right.$$

$$\left. + B_x\frac{\delta\Gamma^{n+1/2}}{\delta p} + B_y\frac{\delta\Gamma^n}{\delta q}\right) + \beta^n \quad (18a)$$

and

$$\frac{\Gamma^{n+1} - \Gamma^{n+1/2}}{\Delta\tau/2} + A_xu^{n+1/2}\frac{\delta\Gamma^{n+1/2}}{\delta p} + A_yv^{n+1/2}\frac{\delta\Gamma^{n+1}}{\delta q}$$

$$= \alpha\left(A_x^2\frac{\delta\Gamma^{n+1/2}}{\delta p^2} + A_y^2\frac{\delta\Gamma^{n+1}}{\delta q^2}\right.$$

$$\left. + B_x\frac{\delta\Gamma^{n+1/2}}{\delta p} + B_y\frac{\delta\Gamma^{n+1}}{\delta q}\right) + \beta^{n+1/2}, \quad (18b)$$

where the time derivatives have been approximated by a simple Euler step.

The nonlinear convective terms cause the main difficulties in separation in order to achieve a stable numerical method. This can be overcome by using the second-upwind-differencing-method, Lilly [42]. One obtains

$$\left(A_xu\frac{\delta\Gamma}{\delta p}\right)^{n+1/2}_{i,j} \approx A_x(i) \cdot [(u_R^n - |u_R^n|)\Gamma^{n+1/2}_{i+1,j}$$

$$\approx A_x(i) \cdot [(u_R^n - |u_R^n|)\Gamma^{n+1/2}_{i+1,j}$$

$$+ (u_R^n + |u_R^n| - u_L^n + |u_L^n|)\Gamma^{n+1/2}_{i,j}$$

$$- (u_L^n + |u_L^n|)\Gamma^{n+1/2}_{i-1,j}]/4\Delta p, \quad (19a)$$

where

$$u_R = u_{i+1,j} + u_{i,j},$$

$$u_L = u_{i,j} + u_{i-1,j},$$

and

$$\left(A_yv\frac{\delta\Gamma}{\delta q}\right)^n_{i,j} \approx A_y(j) \cdot [(v_R^n - |v_R^n|)\Gamma^n_{i,j+1}$$

$$+ (v_R^n + |v_R^n| - v_L^n + |v_L^n|)\Gamma^n_{i,j}$$

$$- (v_L^n + |v_L^n|)\Gamma^n_{i,j-1}]/4\Delta q, \quad (19b)$$

where

$$v_R = (v_{i,j+1} + v_{i,j}),$$

$$v_L = (v_{i,j} + v_{i,j-1}).$$

The second derivatives of the diffusion terms are approximated by centered space evaluation with an error of $O(\Delta x^2)$,

$$\left(A_x^2\frac{\delta^2\Gamma}{\delta p^2}\right)^{n+1/2}_{i,j} \approx A_x^2(i)$$

$$\cdot (\Gamma^{n+1/2}_{i+1,j} - 2\Gamma^{n+1/2}_{i,j} + \Gamma^{n+1/2}_{i-1,j})/\Delta p^2, \quad (20a)$$

$$\left(A_y^2\frac{\delta^2\Gamma}{\delta q^2}\right)^n_{i,j} \approx A_y^2(j)$$

$$\cdot (\Gamma^n_{i,j+1} - 2\Gamma^n_{i,j} + \Gamma^n_{i,j-1})/\Delta q^2. \quad (20b)$$

The first derivatives of the 'diffusion terms', a consequence of the transformation, are also approximated by centered space evaluation but not given here.

The buoyancy term is again approximated by centered space evaluation but with temperatures at time level n and $n + \frac{1}{2}$, respectively. This procedure has a strong stabilizing effect on the overall numerical method. Hence,

$$\left(A_x\frac{\delta\theta}{\delta p}\right)^n_{i,j} \approx A_x(i) \cdot (\theta^n_{i+1,j} - \theta^n_{i-1,j})/2\Delta p. \quad (21)$$

Substituting these approximations into (18a) and (18b) and rearranging the equations one obtains finally for the x-component

$$R^n_{i,j} \cdot \Gamma^{n+1/2}_{i-1,j} + S^n_{i,j} \cdot \Gamma^{n+1/2}_{i,j} + T^n_{i,j} \cdot \Gamma^{n+1/2}_{i+1,j} = U^n_{i,j}$$

$$(22a)$$

and for the y-component

$$R^{n+1/2}_{i,j} \cdot \Gamma^{n+1}_{i,j-1} + S^{n+1/2}_{i,j} \cdot \Gamma^{n+1}_{i,j}$$

$$+ T^{n+1/2}_{i,j} \cdot \Gamma^{n+1}_{i,j+1} = U^{n+1/2}_{i,j}. \quad (22b)$$

These equations are valid for every nod $\{i, j\}$. Given a line with N grid points one obtains for every line j a tridiagonal matrix of size $(N - 2) \cdot (N - 2)$. The same is analogically true for every row i. A schematic diagram of the procedure is given in Fig. 1. Due to the favourable separation process with the 5 point basic grid no auxiliary points outside the boundaries are needed.

3.1.2. *Stability criteria of the ADI-method.* The time step $\Delta\tau$ and the mesh sizes Δx and Δy have to be chosen in such a way that all coefficients of the finite difference equation are positive and that the principal diagonal is still dominant. Richtmyer and Morton [22] have

shown that these criteria are sufficient to achieve a stable numerical method. The first condition is satisfied by introducing the second upwind differencing method [23]. In addition, this method has the advantage that the convection terms, which count for numerical instability, can be physically interpreted. Thereby, a physical quantity enters a control volume with the linear mean velocity of the flow in the direction of the flow.

The second criteria requires that some norm of the matrix is less than unity, Schwarz [24]. The dominance of the principal diagonal is also ensured if the cell-Reynolds number is less than 2 (Thoman and Szewczyk [25]). These last two conditions are identical, but result from different physical reasoning, Roache [16]. The cell-Reynolds number may be obtained from the simplified equation

$$\frac{\partial \Gamma}{\partial \tau} + A_x u \frac{\partial \Gamma}{\partial x} = \alpha A_x^2 \frac{\partial^2 \Gamma}{\partial x^2} + \alpha B_x \frac{\partial \Gamma}{\partial x} + \frac{\partial f(x,y)}{\partial y}.$$

(23)

Analogous to the procedure outlined above one obtains from (23) for the elements of the tridiagonal matrix

$$\Gamma_{i+1} : (u \cdot A_x - \alpha \cdot B_x) \frac{1}{2\Delta x} - \alpha \cdot A_x^2 \cdot \frac{1}{\Delta x^2},$$

$$\Gamma_i : \frac{2}{\Delta \tau} + 2\alpha \cdot A_x^2 \cdot \frac{1}{\Delta x^2},$$ (24)

$$\Gamma_{i-1} : -(u \cdot A_x - \alpha \cdot B_x) \frac{1}{2\Delta x} - \alpha \cdot A_x^2 \cdot \frac{1}{\Delta x^2}.$$

The demand for positive coefficients gives

$$(u \cdot A_x - \alpha \cdot B_x) \cdot \frac{1}{2\Delta x} - \alpha \cdot A_x^2 \cdot \frac{1}{\Delta x^2} > 0 \quad (25)$$

and, hence, one obtains for the cell-Reynolds number

FIG. 1. Schematic diagram of the numerical solution method.

$$Re_x \equiv \frac{u \cdot A_x - \alpha \cdot B_x}{\alpha \cdot A_x^2} \Delta x < 2, \qquad (26)$$

which, for the nontransformed equations, becomes

$$Re_x \equiv \frac{u \cdot \Delta x}{\alpha} < 2. \qquad (26a)$$

One should keep in mind that u and Δx are dimensionless values. Furthermore, the cell-Reynolds number is equal to 4 for two-dimensional problems (Roache [16]). But due to the time splitting equations (22a) and (22b) are essentially one-dimensional which requires $Re_x < 2$.

If (26) is taken to fix the mesh size Δx the permissible time step $\Delta \tau$ follows then from the demand for a dominant principal diagonal.

3.2. Poisson equation

The Poisson equation must be solved twice for each time step. The velocity components u and v are then derived from the definition of the stream function ψ. This immediate 'pull-off' of the velocity components is of essential significance for the exact determination of transient processes. Other methods, as the evaluation of $u^{n+1/2}$ and $v^{n+1/2}$ via extrapolation from u^n, v^n and u^{n-1}, v^{n-1} or the 'drop back' of the velocity components at a full time step have also been studied but are found to be much less efficient (Briley [26], Aziz et al. [27]).

Approximation of (14) through centered space evaluation yields

$$-\omega_{i,j}^n = A_x^2(i) \cdot [\psi_{i+1,j}^n - 2\psi_{i,j}^n + \psi_{i-1,j}^n]/\Delta p^2$$
$$+ A_y^2(j) \cdot [\psi_{i,j+1}^n - 2\psi_{i,j}^n + \psi_{i,j-1}^n]/\Delta q^2$$
$$+ B_x(i) \cdot [\psi_{i+1,j}^n - \psi_{i-1,j}^n]/2\Delta p$$
$$+ B_y(j) \cdot [\psi_{i,j+1}^n - \psi_{i,j-1}^n]/2\Delta q. \qquad (27)$$

This form is based on the well known 5 point grid [28] and has a truncation error of $O(\Delta x^2)$.

The Gauss–Seidel iteration method is properly the best known method to solve (27) (Zurmühl [29]). This iteration process is usually truncated if the difference of the results of two following iterations steps is less than a certain limit

$$|\psi_{i,j}^{n+1} - \psi_{i,j}^n| \leqslant \varepsilon.$$

Extensions of the Gauss–Seidel method are the method by Southwell [30] and some relaxation methods. Thereby, the iteration process is considerably accelerated if an optimum value of the relaxation parameter, $\Omega \lesssim 1$ is used (under or over relaxation). On the other hand, the iteration process is also precipitated by formulating the problem as a pseudo-transient one, i.e. adding an artificial time-dependent term $\partial \psi / \partial \tau^*$. The differential equation is then integrated with respect to this artificial time until a steady state solution is achieved. This integration can be carried out using the already discussed Euler (explicit) or ADI-method (implicit).
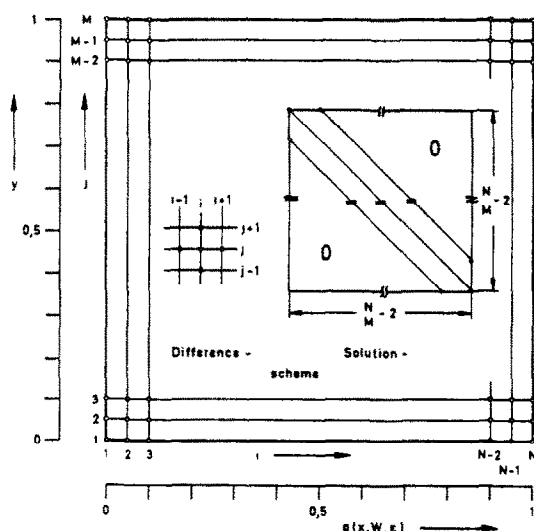
Due to intensive research in recent years direct inversion methods are now coming into use. These methods are extremely accurate. They need considerably less computation time and are, compared to common ADI-methods, more than 20 times faster. A review of known direct inversion methods is given by Dorr [31] whereas Schumann [32] reviews fast elliptic solvers which have been developed very recently.

Some of these methods are limited with respect to suitable boundary conditions and/or the number of grid points in both coordinate directions, but all of them invert the basic pentagonal matrix in an extremely short time.

It appears to us that a reasonable compromise between the necessary computation time, the optimal freedom with respect to boundary conditions and the suitable number of grid points is obtained with the method of cyclic reduction by Schumann and Sweet [33, 34] which solves the general Poisson equation

$$a(x)\frac{\partial^2 \Gamma}{\partial x^2} + b(x)\frac{\partial \Gamma}{\partial x} + c(x)\,\Gamma + \frac{\partial^2 \Gamma}{\partial y^2} = f(x, y). \quad (28)$$

For instance, the subroutine POISSX inverts a matrix with 128×33 grid points in about $0.3\,\text{s}$. Due to the special form of (28) the original pentagonal matrix with unsymmetric side-diagonals is converted into a symmetric tridiagonal matrix. The elements of this tridiagonal matrix are again tridiagonal matrices whereas the side-diagonals are occupied with unit matrices. It is this reduction process which leads to the fast inversion of the original matrix. Further details may be found by Schumann [32].

3.3. *A transformation equation*

Using transformation equations $p(x)$ and $q(y)$ the x and y coordinate can be separately transformed. However, fast Poisson solvers are restricted to equations of the same type as (28) and therefore allow transformation with respect to one of the coordinates
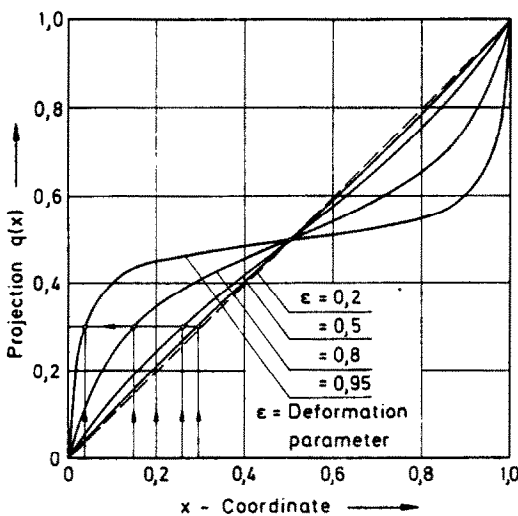
only. Even though this is a limitation of the method, it can be easily met for many problems, especially boundary layer flows.

For free convection in cavities we recommend the relation

$$p(x) = \frac{S}{2}\left[1 + \tan\left[\frac{\pi}{2}\left(\frac{2x}{S} - 1\right)\varepsilon\right]\middle/ \tan\left(\frac{\pi}{2}\varepsilon\right)\right]. \quad (29)$$

Figure 2 shows a graph of this equation for various values of the deformation parameter ε where the optimum of ε is a function of the ratio length to width of the cavity. The parameter S allows the linear transformation of shallow cavities with $W/H \gg 1$ into square ones.

4. APPLICATIONS

The numerical procedure described in Chapter 3 has been tested by determining the solutions for some already known problems. For instance, the governing equations reduce to those describing one- and two-dimensional transient heat conduction problems by setting $Gr = 0$ and $\psi \equiv 0$. The deviation from known analytical solutions is less than 0.1% as test runs have indicated. Furthermore, the predicted thermo- and hydrodynamical entrance flow between parallel plates is accurate to within 1%, compared to the solution given by Schlichting [35]. Finally, the calculated velocity and temperature profiles for free convection flow in vertical gaps deviates from the analytical solution by Bird et al. [17] by less than 0.5%.

In addition, the steady state solution for the problem considered in Chapter 4.1 has been recalculated using the computation method by Gosman [37]. Both results are in agreement to at least 6 decimal places for $Ra < 10^3$. No comparison was possible for higher Rayleigh numbers as the procedure by Gosman did not converge.

We conclude from the results of these test runs that the numerical method described in this paper is highly accurate and especially suitable for free convection problems.

4.1. *Free convection in a square box with different but uniform side wall temperatures*

We consider a closed square two-dimensional box which contains a Newtonian fluid, and is shown schematically in Fig. 3. The side walls are held at different but uniform temperatures T_c and T_h, with $T_c < T_h$. The top and bottom are insulated, and all surfaces are rigid non-slip boundaries. The initial temperature is constant throughout the box and equal to $\theta_0 = 0.5$. At $\tau = 0$, the temperature of the left sidewall falls suddenly to $\theta_c = 0$ and that of the right sidewall rises to $\theta_h = 1$. Both temperatures remain at this new level for ever.

The appropriate governing equations for this problem, subject to the usual Boussinesq approximation, are those given in the previous chapters.

For non-slip boundaries it follows immediately

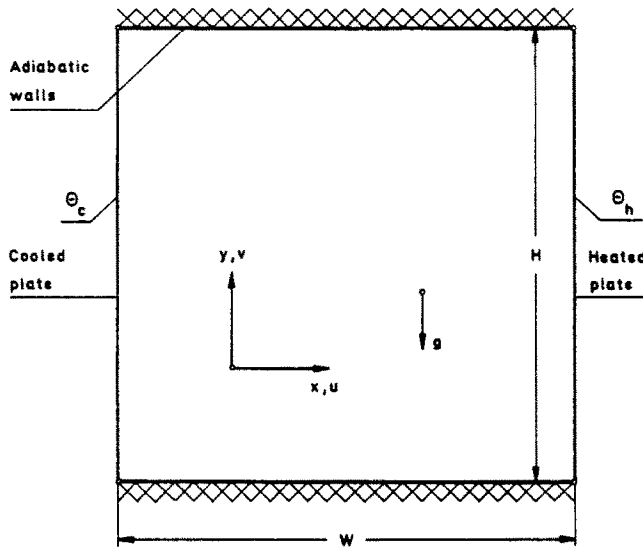FIG. 2. The transformation relation $q(x;\varepsilon)$ for different values of the deformation parameter.

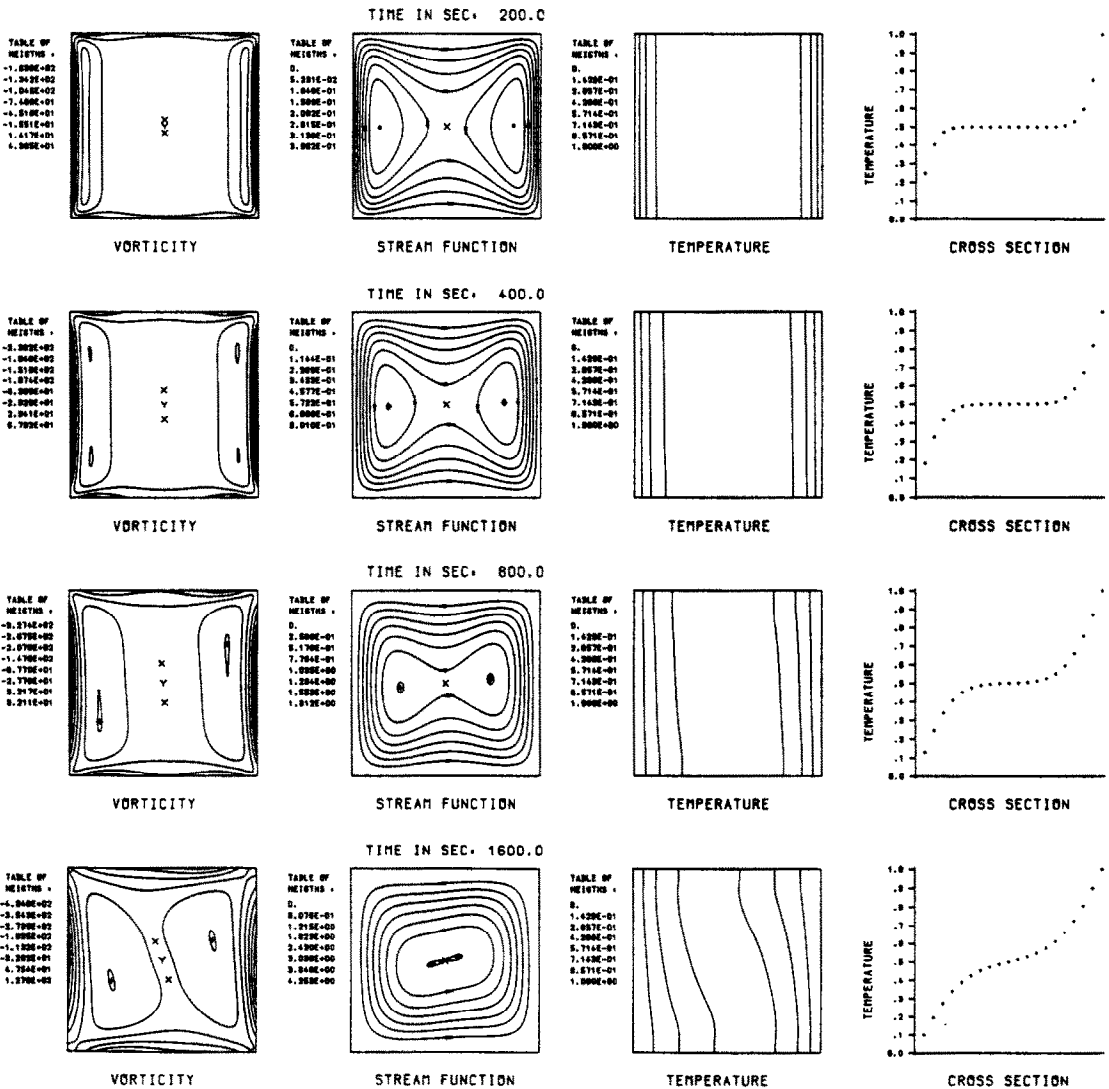FIG. 3. Schematic diagram of example 1.

FIG. 4(a). Transient vorticity, stream-function and temperature patterns at time $t = 200, 400, 800$ and 1600 s, for $Pr = 0.733$ and $Gr = 2 \times 10^4$.
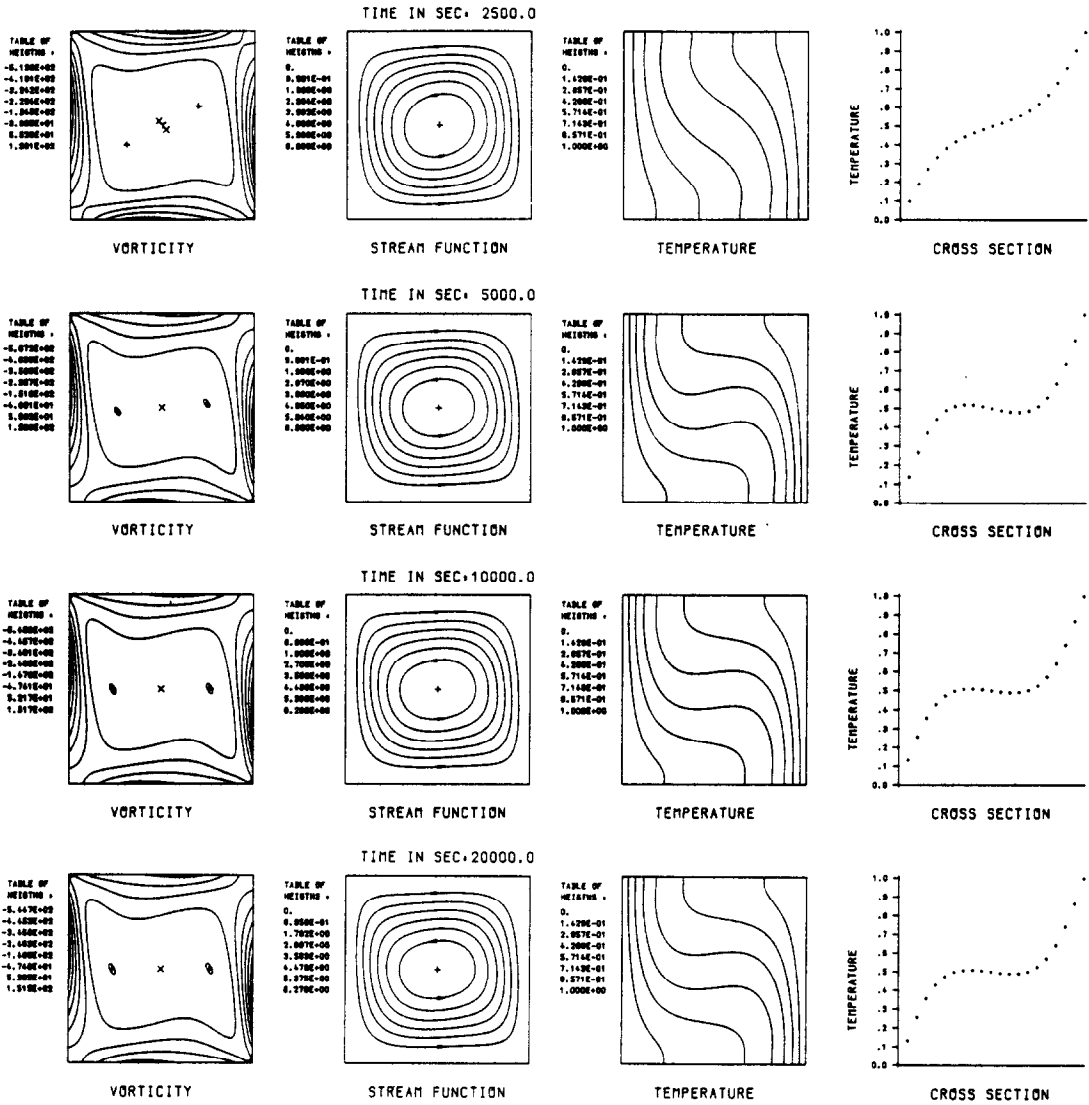
Fig. 4(b). Transient vorticity, stream-function and temperature patterns at time $t = 2500, 5000, 10\,000$ and $20\,000\,s$, for $Pr = 0.733$ and $Gr = 2 \times 10^4$.

from (5) that ψ = const. The vorticity at a non-slip boundary is obtained by a Taylor series out from the wall and is independent of the wall orientation [16],

$$\omega_w = -\frac{2(\psi_{w+1} - \psi_w)}{\Delta n^2} \rightarrow -\frac{2\psi_{w+1}}{\Delta n^2}. \quad (30)$$

Although the truncation error of (30) is $O(\Delta n)$, the resulting numerical procedure is essentially more stable, as it would be with the boundary condition by Woods [36]

$$\omega_w = -\frac{3\psi_{w+1}}{\Delta n^2} + \tfrac{1}{2}\omega_{w+1} \quad (31)$$

which is accurate to $O(\Delta n^2)$.

The adiabatic wall is not represented by the usually used reflection of grid points at the wall, but rather by setting $\theta_w = \theta_{w+1}$. Hence, the heat capacity of a layer with thickness of half a mesh size is neglected. This may

be accepted if a sufficiently large number of grid points is used (Gosman [37]).

The calculations were carried out using 21×21 grid points. The Grashof number has been chosen equal to 2×10^4 and the time step equal to 2 s. The predicted vorticity, stream-function and temperature patterns are shown in Figs. 4 and 5, respectively for different times and for two Prandtl numbers equal to 0.733 (air) and 6.983 (water).

The steady state solution is approximately approached after 1 h for $Pr = 6.983$ and after 2 h for $Pr = 0.733$. As a result of the symmetrical temperature jump at $\tau = 0$ one observes at first two convection rolls which are growing into the core region with time and finally disappear into one roll.

The core region is horizontally well mixed and vertically stably stratified for $Pr = 6.983$. Both the thermal and hydrodynamic boundary layers become
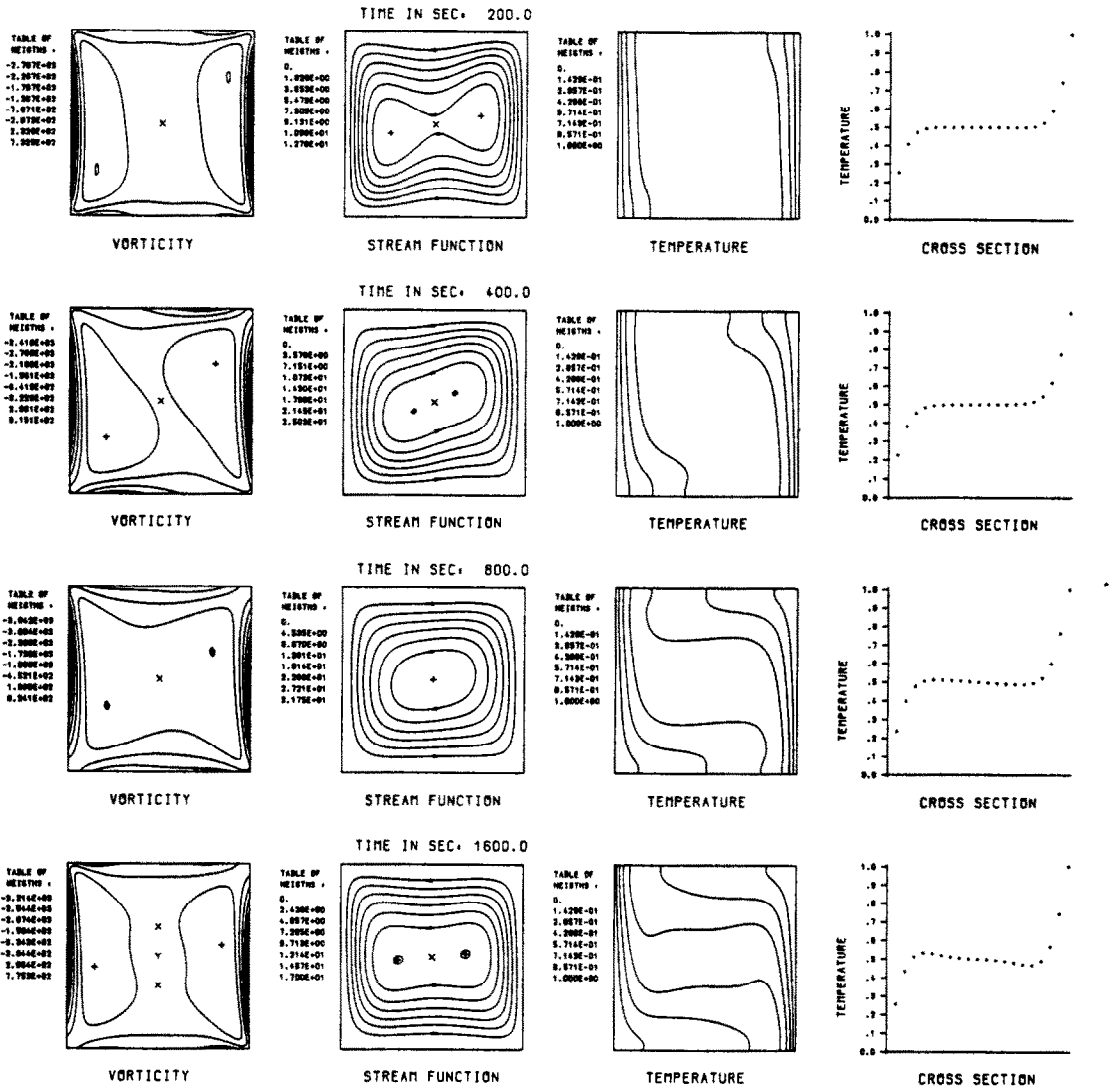
FIG. 5(a). Transient vorticity, stream-function and temperature patterns at time t = 200, 400, 800 and 1600 s, for Pr = 6.983 and Gr = 2 × 10⁴.

thicker with decreasing Prandtl numbers and the temperature profile approaches the conduction solution as $Pr \to 0$ or $Gr \to 0$. It is interesting to note the two maximas in the ψ-pattern at Pr = 6.983 which do not appear at Pr = 0.733. These maximas yield to a recycling flow half way between top and bottom, and were already predicted by de Vahl Davis [12] and Cormack et al. [38] and experimentally verified by Elder [39] for W/H = 1 and by Merker et al. [40] for W/H = 7.5. Elder has estimated that this recycling flow starts at approximately $Ra \approx 10^5$ which is in excellent agreement with the present results.

Comparing the ψ-patterns at different times shows that the stream function increases at first until reaching a maximum and decreases at larger times; i.e. the effect of the local Grashof number on the flow pattern decreases with time due to mixing and internal temperature balancing.

The convergence behavior of the numerical method is checked by runs with different time steps and mesh sizes. Altering the time step results in minor changes of the transient patterns and has no detectable effect on the steady state solution. Figure 6 shows the absolute error as a function of mesh size (decomposition h). The errors obtained with a 21 × 21 grid are: $\Delta\psi/\psi$ = 0.23, $\Delta\omega/\omega$ = 0.20 and $\Delta\theta/\theta$ = 0.025. The reference point for these errors and the 'exact' solution can be estimated if numerical solutions with three different mesh sizes are known. These are shown below.

Assuming that the steady state solutions $f_{i,j}$ at each grid point (x_i, y_j) converge parabolically to the exact solution $f^*_{i,j}$ with decreasing mesh size, one has for three different mesh sizes where $1/h$ follows a geometrical series

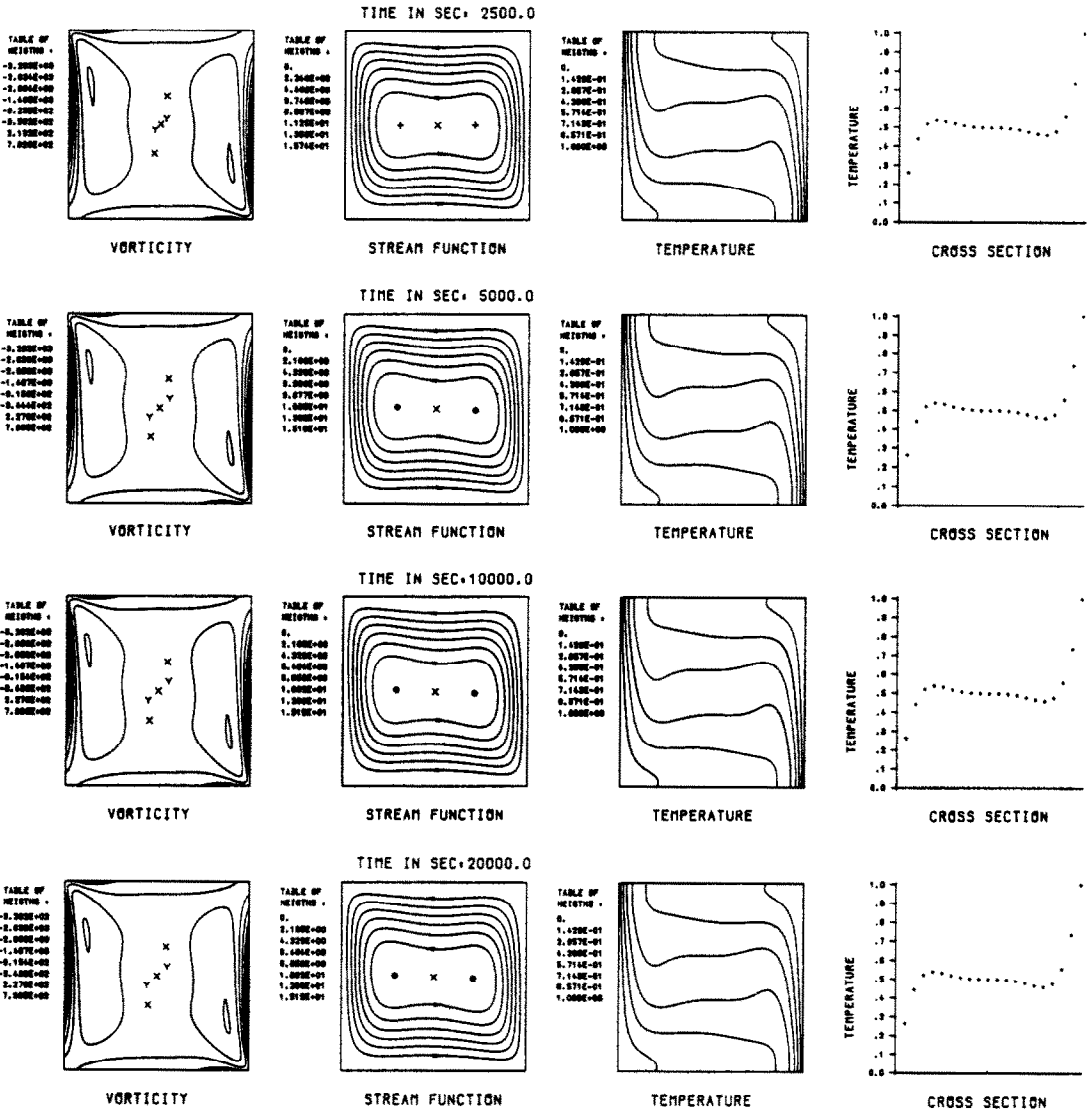| Grid	11 × 11	21 × 21	41 × 41
$1/h$	10	20	40

FIG. 5(b). Transient vorticity, stream-function and temperature patterns at time $t = 2500$, 5000, $10\,000$ and $20\,000$ s, for $Pr = 6.983$ and $Gr = 2 \times 10^4$.

with $q = 1/2$, or

Grid	19×19	31×31	51×51
$1/h$	18	30	50

with $q = 3/5$.

Hence, by neglecting higher order terms

$$f_{10} = f^* + f_k\, h_{10}^k,$$
$$f_{20} = f^* + f_k\, h_{20}^k, \tag{32}$$
$$f_{40} = f^* + f_k\, h_{40}^k.$$

The mesh size or decomposition rates are related

$$h_i = q \cdot h_{i-1}. \tag{33}$$

The difference of the two following solutions is

$$d_1 = f_{20} - f_{10} = f_k h_{10}^k (q^k - 1),$$
$$d_2 = f_{40} - f_{20} = f_k h_{10}^k q^k (q^k - 1). \tag{34}$$

Hence

$$q^k = \frac{d_2}{d_1} \tag{35}$$

and, therefore, for the wanted exponent k

$$k = (\ln(d_2) - \ln(d_1))/\ln(q). \tag{36}$$

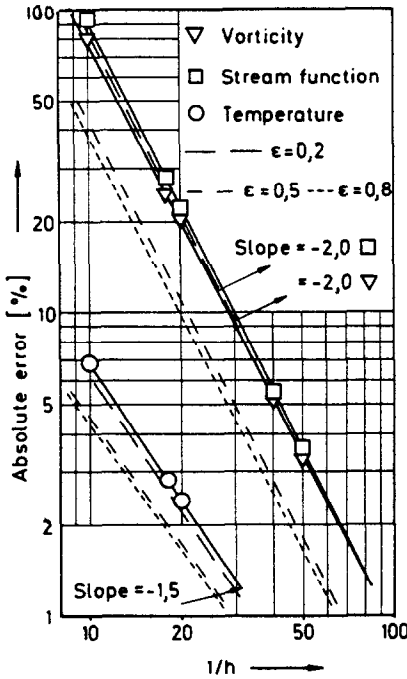The exact solution can now easily be calculated from equation (32).

FIG. 6. Absolute errors vs grid spacing.

FIG. 7. CPU-time, vs number of grid points.

The average error over all grid points is shown in Fig. 6 for different decomposition rates h. It can be seen that the vorticity and stream function converge with exponent $k = 2$, whereas the temperature field converges with $k = 1.5$. The vorticity and stream function show large errors at large mesh size steps whereas the temperature shows relatively small errors even at large mesh sizes. This is in agreement with the well known fact that the temperature field reacts weakly to changes in the flow field. Some transient numerical methods take advantage of this weak dependence and solve the temperature equation every nth time step only.

Figure 6 also shows the results obtained with the transformation relation. Principally, the numerical error decreases with increasing deformation rate ε. As there is practically no effect for $\varepsilon \leqslant 0.2$ one visualizes substantially reduced errors for moderate values, i.e. $\varepsilon \approx 0.5$. Increasing ε further concentrates the number of grid points in the boundary layer region. Since the total number of grid points is constant, only a few points remain in the core region. Hence, as the boundary layer region will be calculated more and more accurately, the core region suffers. Therefore, it is clear that there exists an optimal value for ε which is approximately 0.8 in the present case.

The numerical calculations have been performed on a CDC-Cyber 175. The necessary computation time as a function of the number of grid points is given in Fig. 7. This figure shows that using the transformation relation increases the computation time by approximately 30%. In general, time increases linearly with the number of grid points. This favourable behavior (otherwise quatric or cubic increasing) is due to the ADI-method which is used to integrate the energy and

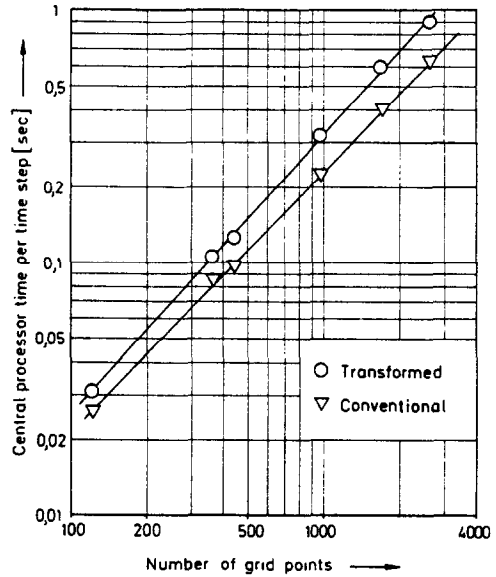vorticity equation. Furthermore, the computation time is approximately equally distributed between the three basic equations as test runs have shown.

4.2. Free convection in a square box with one side wall nonuniformly heated and the other held adiabatic

Again, we consider a closed square and two-dimensional box, but now, only one side wall is heated at its lower half and cooled at its upper with different but uniform temperatures T_h and T_c. On the left side wall, the top and bottom are again insulated and all surfaces are rigid non-slip boundaries. This arrangement can be treated as a crude model of a room heated by a radiator and cooled off by a window (closed!), and is shown schematically in Fig. 8. The initial temperature is constant and equal to unity.

During the first 500 s the temperature of the side wall is maintained uniformly at $\theta_w = 0$. At $t = 500$ s the temperature of the lower half rises suddenly to $\theta_{w,h} = 1$ and remains there for all further times.

Figure 9 shows the predicted vorticity, stream function and temperature patterns for different times and for the case where $Ra = 5.6 \times 10^5$. The upper line represents the patterns after 500 s, which are self-evident and may therefore not be discussed further. After having changed the temperature at the lower half, one finally ends up with a periodic state; i.e. one obtains two convection rolls, one in the upper and one in the lower part of the box. These rolls grow and decay periodically with time, as is shown in the second and third line of Fig. 9. The diagrams show approximately the maximum and minimum size of the rolls. A similar behavior has been observed by Igarashi [41] who studied free convection in a square box due to a line source at the bottom. We do not feel that this periodic state is a direct consequence of our limitation to a two-dimensional box. Taking three-dimensional effects
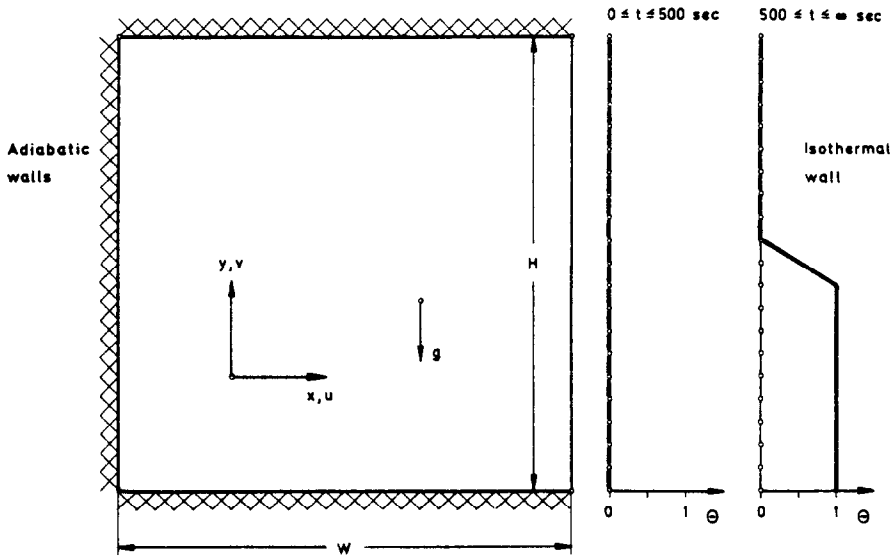
FIG. 8. Schematic diagram of example 2.

into account may alter the periodic state but does not let it disappear. One should notice that the vertical density stratification is unstable with a high density fluid above a low density fluid. Therefore, it is most likely that the observed periodic state results from the involved stability problem.

Figure 10 shows the frequency of oscillations as a function of the Rayleigh number. The calculated frequencies follow the parabolic relation very closely

$$f/f_0 = \sqrt{Ra/Ra_0}. \qquad (37)$$

The numerical calculations for this example have been carried out with a 21×21 grid but without utilization of the transformation relation.
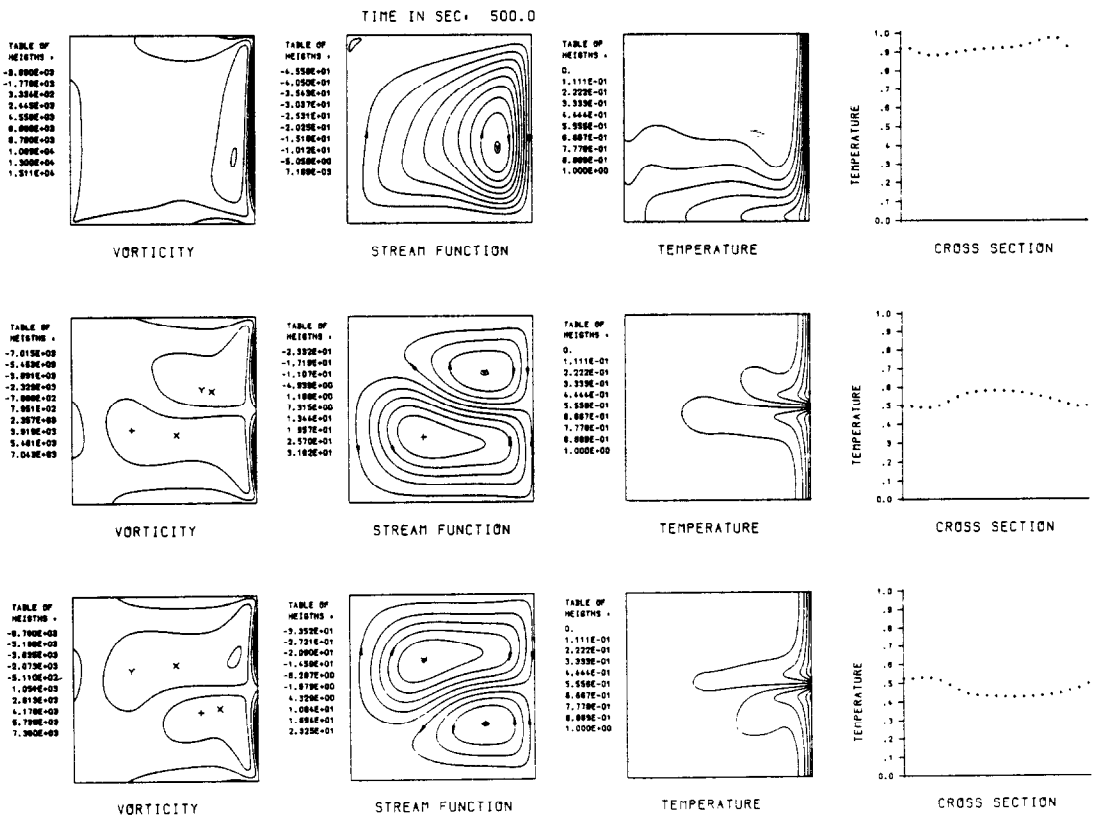

FIG. 9. Transient vorticity, stream-function and temperature patterns at different times.
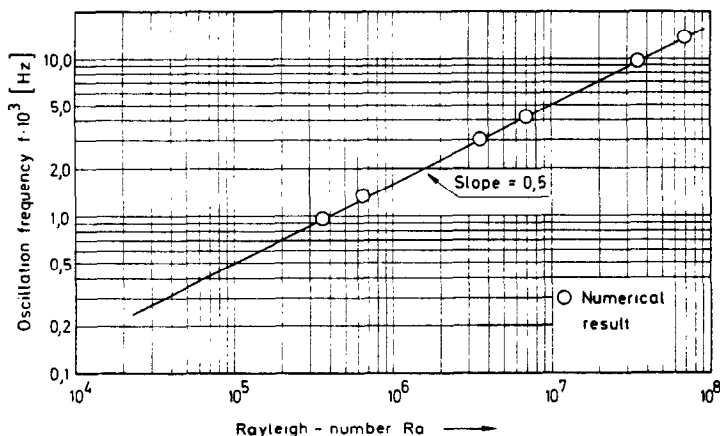
FIG. 10. Oscillation frequency vs Rayleigh number.

5. CLOSING COMMENTS

The numerical method described in this paper has some benefits compared to already known procedures. Through the adaptation of the ADI-method for the vorticity and energy equation and of the method of cyclic reduction for the Poisson equation, it has become possible to study extremely slow transient processes. Test runs have shown that the computation time necessary to simulate free convection in closed containers of moderate size (volume 1 m^3) over a time period of approximately 5 days is somewhat below 1 h. Furthermore, the method is applicable to Rayleigh numbers up to 10^{12}. This is essentially due to the use of the method of second upwind differencing. The method of fast cyclic reduction used to integrate the Poisson equation calculates the velocity components at every half time step. This procedure increases the accuracy of transient solutions considerably. The transformation relation previously discussed is extremely useful in cavity problems with boundary layers at the vertical walls. Finally, the flow area has not necessarily been restricted to rectangular cavities. More general geometries can be treated by introducing well-chosen running statements for the dummy running indices.

However, it should be kept in mind that the present method is restricted to laminar flow. Therefore, it should be carefully checked whether the considered flow is still laminar or already turbulent as the Rayleigh number approaches higher values. If the temperature differences are small but the geometrical dimensions of the cavity are large the observed flow may be still laminar even at high Rayleigh numbers.

REFERENCES

1. G. Schöll, Warmwasser-Großwärmespeicher, VDI-Berichte 223, 33–38 (1976).
2. J. Straub, G. Merker, K. Küblbeck, A. Staudt and U. Grigull, Untersuchung der Konvektion in Jahres-

wärmespeichern, VDI-Berichte 288, 39–46 (1977).
3. W. Moog, Theoretical considerations of similarity for air flow within the open space, Klima Kälteingenieur, Jg. 6, Heft 11 (1978).
4. S. Bloß, Temperaturverteilung in Seen, Dissertation, TU München, Germany (1977).
5. G. Poots, Heat transfer by laminar free convection in enclosed plane gas layers, Q. J. Mech. appl. Math. 9, 257–273 (1958).
6. M. van Dyke, Perturbation Methods in Fluid Mechanics. Parabolic Press, Stanford, California, U.S.A. (1975).
7. A. Nayfeh, Perturbation Methods. Wiley-Interscience, New York (1973).
8. D. E. Cormack, L. G. Leal and J. Imberger, Natural convection in a shallow cavity with differentially heated and walls — I. Asymptotic theory, J. Fluid Mech. 65, 209–229 (1976).
9. A. Rubel and E. Landis, Numerical study of natural convection in a vertical rectangular enclosure, High-Speed Comp. Fluid Dyn., Phys. Fluids Suppl. II, 208–213 (1969).
10. J. E. Fromm, Practial investigations of convective difference approximations of reduced dispersion, High-Speed Comp. Fluid Dyn., Phys. Fluids Suppl. II, 3–12 (1969).
11. J. E. Fromm, Numerical method for computing nonlinear, time-dependent, buoyant circulation of air in rooms, IBM J. Res. Develop. 5, 186–196 (1971).
12. G. de Vahl Davis, Laminar natural convection in an enclosed rectangular cavity, Int. J. Heat Mass Transfer 11, 1675–1693 (1968).
13. R. K. MacGregor and A. F. Emery, Free convection through vertical plane layers — moderate and high Prandtl number fluids. J. Heat Mass Transfer, Trans. ASME 91C, 391–403 (1969).
14. J. Wilkes, The finite difference computation of natural convection in an enclosed rectangular cavity, Ph.D. Thesis, University of Michigan (1963).
15. K. E. Torrance, Comparison of finite element computation of natural convection, J. Res., NBS 72B, (1968).
16. P. J. Roache, Computational Fluid Dynamics. Hermosa, Albuquerque, U.S.A. (1976).
17. R. B. Bird, W. E. Stewart and E. N. Lightfoot, Transport Phenomena. John Wiley, New York (1960).
18. F. M. White, Viscous Fluid Flow. McGraw-Hill, New York (1974).
19. J. Stoer and R. Bulirsch, Einführung in die Numerische Mathematik I & II. Springer-Verlag, Berlin (1973).
20. D. W. Peaceman and H. H. Rachford, The numerical solution of parabolic and elliptic differential equations, J. Soc. Indust. appl. Math. 3(1), 28–41 (1955).
21. A. S. Householder, The Theory of Matrices in numerical Analysis. Blaisdell, New York (1964).

22. R. D. Richtmyer and K. W. Morton, *Difference Methods for the Initial-Value Problems*, 2nd Edn. Interscience, New York (1967).
23. R. A. Gentry, R. E. Martin and B. J. Daly, An Eulerian differencing method for unsteady compressible flow problems, *J. Comput. Phys.* **1**, 87–118 (1966).
24. H. R. Schwarz, H. Rutishauser and E. Stiefel, *Matrizen — Numerik*. Teubner, Stuttgart (1968).
25. D. C. Thoman and A. A. Szewczyk, Numerical solutions of time dependent two-dimensional flow of a viscous, incompressible fluid over stationary and rotating cylinders, Tech. Rept. 66-14, University of Notre Dame, Indiana (1966).
26. W. R. Briley, A numerical study of laminar separation bubbles using the Navier–Stokes-equations, Rep. J110 614-1, United Aircraft Research Lab., East Hartford, Connecticut.
27. K. Aziz and J. D. Hellums, Numerical solution of the three-dimensional equations of motion for laminar natural convection, *Phys. Fluids* **10**(2), 314–324 (1967).
28. G. D. Smith, *Numerische Lösung von partiellen Differentialgleichungen*. Vieweg, Braunschweig (1970).
29. R. Zurmühl, *Praktische Mathematik*. Springer-Verlag, Berlin (1957).
30. R. V. Southwell, *Relaxation Methods in Theoretical Physics*. Oxford University Press, New York (1946).
31. F. W. Dorr, The direct solution of the discretized Poisson equation on a rectangle, *Siam Rev.* **12**, 248–263 (1970).
32. U. Schumann, Fast elliptic solvers, *Proc. GAMM-Workshop on Fast Solution Methods for the discretized Poisson equation*. Advance Publications, Karlsruhe

(1977).
33. U. Schumann and R. A. Sweet, A direct method for the solution of Poisson's equation with Neumann boundary conditions on a staggered grid of arbitrary size, *J. Comput. Phys.* **20**, 171–182 (1976).
34. U. Schumann and R. A. Sweet, Direct Poisson equation solver for potential and pressure fields on a staggered grid with obstacles, *5th Int. Conf. Numer. Meth. in Fluid Dyn., Lecture Notes in Phys.* **58**, 398–403 (1976).
35. H. Schlichting, *Grenzschicht-Theorie*. Verlag G. Braun, Karlsruhe 2. Aufl. (1964).
36. L. C. Woods, A note on the numerical solution of fourth order differential equations, *Aeronaut. Q.* **5**(3), (1954).
37. A. D. Gosman, W. P. Pun, A. K. Runchal, D. B. Spalding and M. Wolfshtein, *Heat and Mass Transfer in Recirculating Flows*. Academic Press, London (1969).
38. D. E. Cormack, L. G. Leal and J. H. Seinfeld, Natural convection in a shallow cavity with differentially heated end walls — II. Numerical solutions. *J. Fluid Mech.* **65**, 231–246 (1974).
39. J. W. Elder, Laminar free convection in a vertical slot, *J. Fluid Mech.* **23**(1), 77–98 (1965).
40. G. P. Merker and U. Grigull, Freie Konvektion in einem flachen Behälter mit und ohne Rotation. *Wärme- u Stoffübertr.* **8**, 101–112 (1975).
41. T. Igarashi, Natural convective oscillatory flow in an enclosed space, *Bull. ISME* **21**(156) (1978).
42. D. K. Lilly, On the computational stability of numerical solutions of time-dependent non-linear geophysical fluid dynamics problems, *Monthly Weather Rev.* **93**(1), 11–26 (1965).

CALCUL NUMERIQUE DE CONVECTION NATURELLE BIDIMENSIONNELLE ET VARIABLE DANS LE TEMPS, A L'INTERIEUR DE CAVITES

Résumé – On développe une méthode de calcul numérique pour déterminer la convection naturelle laminaire à deux dimensions et variable dans le temps pour des cavités fermées, et de la convection forcée dans les tubes et les cavités ouvertes. Les équations de transport de l'énergie et du tourbillon sont résolues à l'aide de la méthode ADI, mais la méthode la plus récente de réduction cyclique est appliquée à l'équation de Poisson. La méthode implicite résultante est stable jusqu'à un nombre de Rayleigh de 10^{12}. A cause d'un grand pas de temps possible, la méthode est particulièrement qualifiée pour des problèmes transitoires avec des propriétés changeant lentement. Une transformation $q\,(x, \varepsilon)$ est proposée pour la détermination assez précise des couches limites thermique et hydrodynamique près des parois verticales des cavités. L'intérêt de cette technique numérique est illustré en résolvant deux problèmes de convection naturelle dans une cavité rectangulaire, avec des parois chauffées différenment mais uniformément et avec une seule paroi chauffée non uniformément.

NUMERISCHE BERECHNUNG ZWEIDIMENSIONALER, ZEITABHÄNGIGER FREIER KONVEKTION IN HOHLRÄUMEN NACH EINER FORTGESCHRITTENEN METHODE

Zusammenfassung – Eine zweidimensionale, zeitabhängige numerische Rechenmethode wurde entwickelt, um die laminaire freie Konvektion in geschlossenen Hohlräumen und erzwungene Konvektion in Leitungskanälen und offenen Hohlräumen zu bestimmen. Die Transportgleichungen für die Energie- und Wirbelfunktion werden mit Hilfe der ADI-Methode gelöst, auf die Poisson-Gleichung jedoch wird die erst vor kurzem entwickelte Methode der zyklischen Reduktion angewandt. Die resultierende implizite Methode bleibt bis zu einer Rayleigh-Zahl von 10^{12} stabil. Infolge des zulässigen großen Zeitschritts ist die Methode besonders für instationäre Probleme mit extrem langsam veränderlichen Werten geeignet. Eine Transformationsbeziehung $q(x, \varepsilon)$ wird zur ausreichend genauen Bestimmung der thermischen und hydrodynamischen Grenzschichten vorgeschlagen. Der Nutzen der beschriebenen numerischen Rechentechnik wurde bei der Lösung von zwei Problemen freier Konvektion in einem rechteckigen Hohlraum demonstriert, wobei einmal die Seitenwände unterschiedlich, aber gleichmäßig, beheizt waren und einmal nur eine Seitenwand ungleichmäßig beheizt wurde.

УСОВЕРШЕНСТВОВАННЫЙ ЧИСЛЕННЫЙ РАСЧЁТ ДВУХМЕРНОЙ НЕСТАЦИОНАРНОЙ СВОБОДНОЙ КОНВЕКЦИИ В ПОЛОСТЯХ

Аннотация — Разработан двухмерный нестационарный численный метод расчёта ламинарной свободной конвекции в закрытых полостях и вынужденной конвекции в каналах и открытых полостях. Уравнения переноса энергии и завихренности решались приближенным разностным методом, а уравнение Пуассона решалось с помощью разработанного сравнительно недавно метода циклической редукции. Полученный в результате неявный метод устойчиво работает вплоть до значений числа Релея $\sim 10^{12}$. Благодаря возможности использования большого шага по времени метод наиболее эффективен для решения нестационарных задач, в которых свойства изменяются крайне медленно. Предложена зависимость $q(x, \varepsilon)$ для достаточно точного определения тепловых и гидродинамических пограничных слоёв у вертикальных боковых стен полостей. Преимущество предложенного численного метода расчёта проиллюстрировано на примере решения двух задач свободной конвекции в прямоугольной полости: с равномерно нагретыми до различных температур боковыми стенками и с одной неравномерно нагретой стенкой.